Transactions of the Japan Welding Society, Vol. 17, No. 1, April 1986

Estimation of Cracking Susceptibility of Nodular Graphite Cast Iron by the Implant Test*

—Study on the Weld Cracking of Nodular Graphite Cast Iron (Report 1)—

By Shosuke ITOMURA, Kenki HESHIKI** and Fukuhisa MATSUDA*****

Abstract

A study on the cracking susceptibility of nodular graphite cast iron by means of the implant test at different heat inputs is described. Most of the implant specimens were 6 mm in diameter and made without notching. Weld heat inputs, with the use of 4 mm diameter DFCNiFe type electrode (55% Ni-Fe), were changed as 1.8, 2.1 and 2.4 kJ/mm with 1.67 mm/sec travel speed and 50 mm bead length. After welding, when the temperature of the HAZ cooled to about 673K, the load was applied.

The implant specimens were fractured at about 373K, which was below the Ms temperature of the cast iron used. In the heat input range of the present study, when the heat input was increased, the lower critical stress of fracture slightly increased; but it went up to only below one half of the strength of the base metal. The implant specimens were fractured at the part of the martensite structure with the highest micro-vickers hardness number, about 900. The fracture surface consisted of mainly intergranular fracture with partly quasi-cleavage fracture mode.

Key Words: Nodular graphite cast iron, Weld cold cracking, Implant test, Martensite transformation start temperature, Lower critical stress, SMA welding

1. Introduction

Cast iron still remains a difficult material to weld though steel welding technology has made great progress in recent years. Cast iron weldings are now mainly employed in repair works and not positively in weld structural works because of the low reliability of the cast iron weld joint. Cast iron welding studies have used various methods such as arc welding[1], electroslag welding[2] and electron beam welding[3]. A successful example of gas welding of nodular graphite cast iron with the filler material of high silicon hyper-eutectic nodular graphite cast iron has also been reported[4]. If we can succeed in getting a reliable enough cast iron weld joint by means of arc weldnig, the most popular process of weld structure, then cast iron may cease to be a difficult material to weld, which is now beset by the problem of weld cracking due to the formation of white cast iron in the fusion zone and martensite in HAZ. Weld cracking is the first problem to be solved for improving the reliability of cast iron weld joint.

In this paper the authors explored the possibility of estimating the cracking susceptibility of nodular graphite cast iron by the implant test. This material was adopted for the test because it has excellent properties such as high strength, ductility, machinability and wear resistance and is used often as a structural member in place of steel.

2. Materials and Experimental Procedure

The base material is nodular graphite cast iron of 590 MPa tensile strength (FCD 60) and the electrode adopted is Fe-Ni base electrode for csat iron (equivalent to JIS DFC NiFe, 4 mm diameter) which is readily available in the general market and is therefore convenient for practical applications. Table 1 shows the chemical compositions and tensile strength of the base metal and the deposited metal. The base metal has a microstructure of "bull's eye", or nodular graphite surrounded by circular ferrite in the pearlite matrix as shown in Fig. 1. Implant specimens are machined to the shape and size shown in Fig. 2 from cast bar deflection test pieces of 30 mm diameter and 500 mm length. The implant specimen usually has a circumferential notch or a spiral notch, but in this experiment the specimens were mainly smoothed specimens 6 mm in diameter. For comparison, 5 pieces each of the smoothed specimens and the circumferential V-shape notched specimens (0.5 mm depth of notch, 5 mm diameter at the notch bottom and 0.1 mm notch tip radius) were subjected to tension tests, and both specimens showed nearly the same mean strength, 605.6 MPa and 606.6 MPa respectively.

A study by Noguchi[5] of the rupture stregnth of round cast iron bar with circumferential notch analyses shows that nodular graphite cast iron changes in

Table 1 Chemical compositions and tensile strength of nodular graphite cast iron used and deposited metal

	Chemical compositions (wt%)							T.S.
	C	Si	Mn	P	S	Mg	Ni	(MPa)
FCD 60	3.55	2.79	0.47	0.024	0.011	0.03	—	605.6
Depo.metal DFCNiFe	0.99	0.28	1.90	0.007	0.002	—	54.34	520

* Received 20 November 1985
** University of the Ryukyus: Nishihara-cho, Okinawa, Japan
*** Osaka University: Suita City, Osaka, Japan

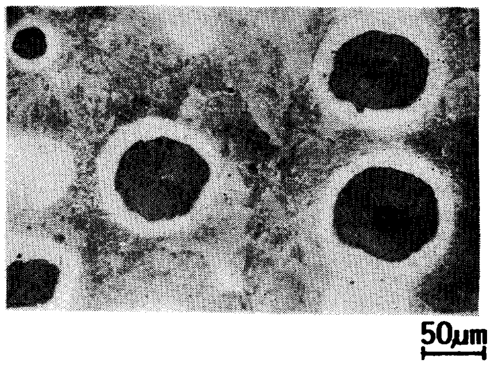

Fig. 1 Microstructure of cast iron used

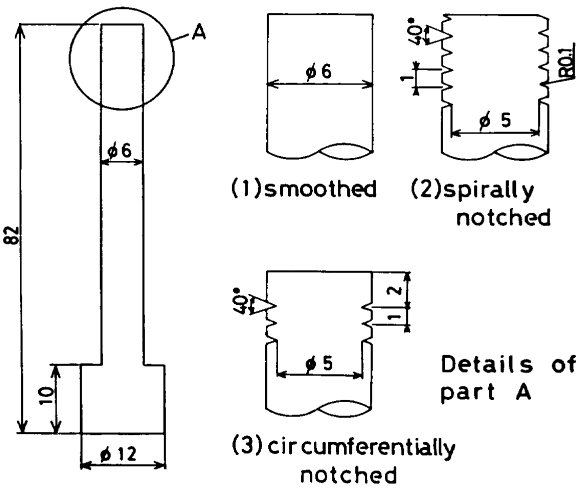

Fig. 2 Size and shapes of implant specimens

strength with notching, the same as steel does. This behavior is different from that of flaky graphite cast iron, which is regarded generally as a material with low sensitivity to notching. In his report the experimental results show about FCD 60 when the elastic stress concentration factor α is up to 2.6, but in the present work the value of α is 7.2. This number is obtained by Neuber's method[6] applied to the size of the notched specimens mentioned above. For this size of notch, the notch effect of tiny nodular graphite grains dispersed in the matrix may be greater than the three-dimensional restriction effect of the notch, and this might lead to no difference in strength between the smoothed and notched specimens. Indeed practically no effect of the notch was found in the results of the implant test as shown later in Fig. 5-B. Fig. 3 shows the size and shape of the backing plate. The mild steel plate (SS 41) is grooved to a depth of 3 mm and drilled with holes to insert the implant specimens so that the bead length becomes 50 mm as the electrode maker recommends. This method permits the test to be made eight times with one backing plate. Granjon[7] reported that the thermal cycle of the implant test specimen coincides with the thermal cycle which is determined by the characteristics of the backing plate when the materials of the test specimen and the backing plate differ from each other. Figure 4 shows the cross sectional macrophotographs of the beads on the same size backing

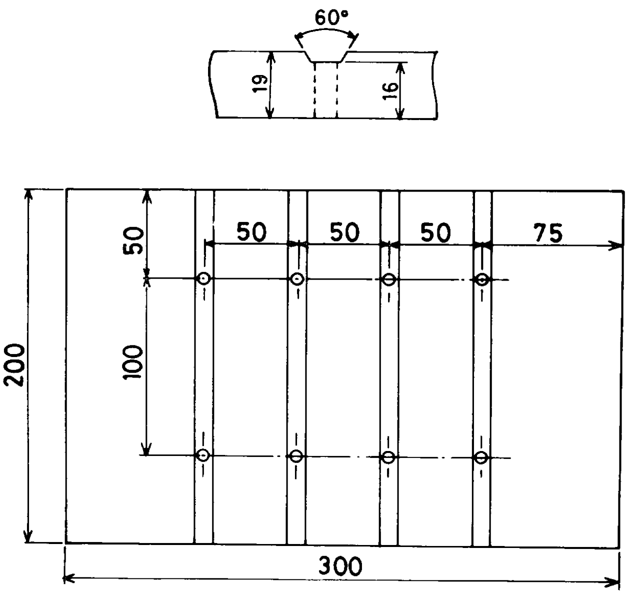

Fig. 3 Size and shape of backing plate

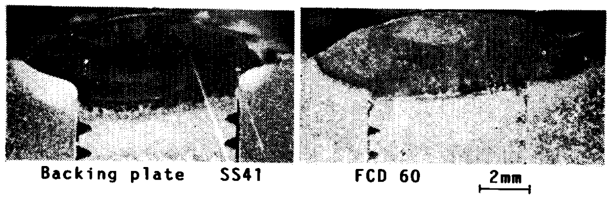

Fig. 4 Macrophotographs of welds, backing plate: SS41 (left), FCD60 (right), heat input: 2.1 kJ/mm

plates of SS 41 and FCD 60 respectively. Though the penetration of the cast iron plate was deeper because of its lower melting point, the penetration of the implant test specimens was almost the same in spite of the difference of backing plates. As mentioned later, all the implant test specimens fractured at HAZ, so the difference in materials between the specimen and the backing plate seemed to pose no problem. As shown in Table 2 the heat input was changed in three stages. The experiments were executed at room temperature without preheating or postheating. To obtain the heat cycle at HAZ, holes were drilled from the bottom side of the backing plate at two points, each 10 mm from the test specimen on both sides along the welding line and almel-chromel thermocouples were inserted into these holes so that the heat sensing points came at the position of the weld bond. Based on the mean thermal cycle obtained after several experiments, the starting time of the test loading was determined and the temperature of HAZ at the time of fracture of the implant specimen was estimated.

Table 3 shows the cooling time from 1073K to 773K at each stage of the heat input. The standard starting

Table 2 Welding conditions

Welding speed	1.67mm/sec		
Bead length	50mm		
Heat input (Welding current)	1.8kJ/mm, 120A	2.1kJ/mm, 140A	2.4kJ/mm 160A

Table 3 Cooling time from 1073K to 773K at partially melted zone

Heat input kJ/mm	Cooling time (sec) 1073K-773K
1.8	3.9
2.1	4.5
2.4	4.9

time of loading was set at 10 seconds after the arc passed the center of the test specimen. At that time the temperature of HAZ was comparatively high, being around 673K. The reason for setting the loading start time at such a high temperature is that the temperature at which the martensite transformation does not yet occur at HAZ is thought to be desirable. This is in accordance with a report[8] which says that the weld crack of high carbon steel is considered a kind of quenching crack due to the martensite transformation. The testing apparatus employed in this study is a lever type tester which applies a load to the test specimen by removing pressure from the oil jack supporting the preset weight. It reaches the set load in 1.5 seconds while the temperature drops about 40K.

3. Experimental Results and Discussion

3.1 *Results of Implant Test*

Figure 5 shows the relation between the applied stress and the temperature of the bond line at the time of fracture at each stage of heat input. Each dot in the diagrams represents a temperature at which the test specimen fractured, and when the specimen did not break until the temperature dropped to 323K, the test was stopped. This is shown by an arrow mark in the diagram. In the case of 2.1 kJ/mm welding heat input (Fig. 5-B), most tests started loading at 683K, but several tests started it below 683K. They are shown by the marks ●▲■ in the diagram. The test results show that circumferential notch specimens and spiral notch specimens fractured in the same range of temperatures, and little difference was found between the smoothed specimens and notched specimens. In all the stages of welding heat input, the specimens fractured at around 373K, regardless of the load starting temperature. There was a tendency to shift to the hotter side as the applied stress increased.

The critical rupture stress increases as the welding heat input increases, but the increment is small, the critical stress for 1.8, 2.1 and .2.4 kJ/mm of heat input being 250, 274 and 290 MPa respectively. The fact that the fracture happens at a constant temperature, around 373K with little variation according to the stress, time and heat input is considered to be related to the quench cracking[9]. For evidence, small test pieces having 3 mm diameter and 10 mm length were machined from the implant test specimens and sub-

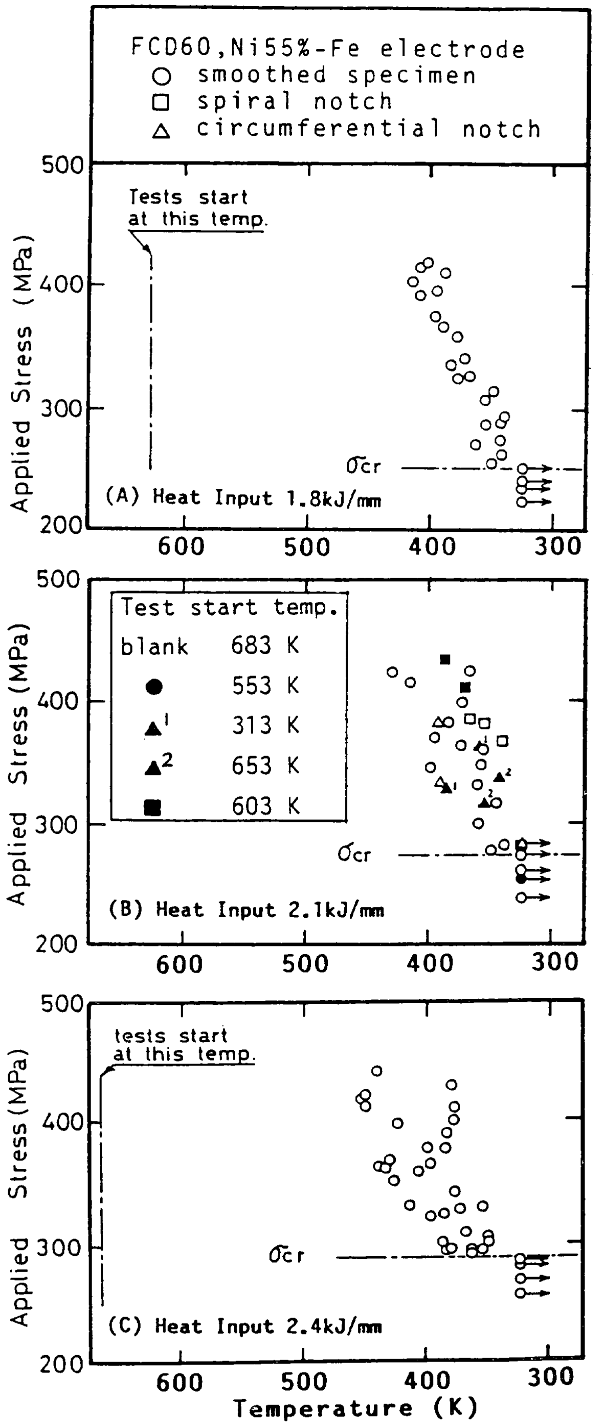

Fig. 5 Results of implant tests, heat input: 1.8 kJ/mm (upper), 2.1 kJ/mm (middle) and 2.4 kJ/mm (lower)

jected to the continuous cooling transformation measuring apparatus to find the martensite transformation start temperature (Ms point), and the result is shown in Fig. 6. The thermal cycle given to this test was the same as that in the implant test on 2.1 kJ/mm heat input (4.5 seconds for cooling from 1073K to 773K), and the maximum heating temperature was altered. The diagram shows a remarkable drop in the Ms point with an increase in maximum heating temperature. This is considered to be due to a difference of carbon diffusion from the graphite grains to the matrix structure during the thermal cycle, and this means

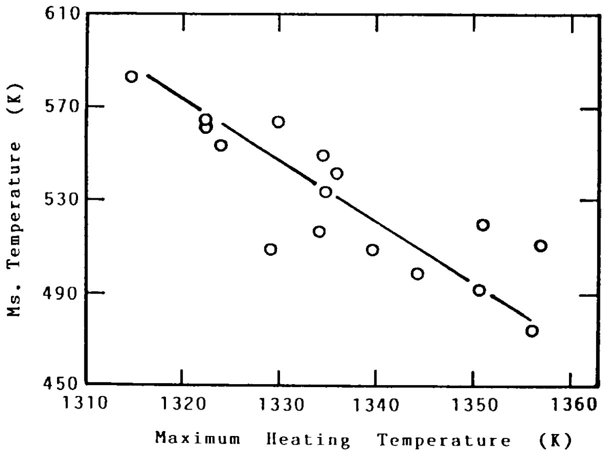

Fig. 6 Relationship between maximum heating temperature and Ms. temperature of cast iron used

that different spots in the welding heat-affected zone of cast iron have different Ms points according to their thermal cycles. The fact that the temperature at which fracture occurs (shown in Fig. 5) is obviously lower than the Ms point (shown in Fig. 6) means that the fracture occurs after the martensite transformation begins to progress on the weld bond line.

3.2 *Structure of Fractured Region*

It has been reported that the welding bond line of cast iron contains a ledeburite structure which is formed from high carbon melt by rapid cooling and is the metastable eutectic structure seen in the Fe-C double diagram. The authors tried to find out the relation between the ledeburite structure and the weld crack of cast iron by means of observation and analysis of the bond line structure according to the suggestion of Savage[10] who proposed a detailed definition of the bond line. The bond line has been loosely defined and used with widely different meanings.

Figure 7 shows a microstructure of the weld region of nodular graphite cast iron subdivided according to the proposal of Savage. In region III, a ledeburite is seen around nodular graphite grain. This ledeburite can be considered a metastable eutectic structure solidified from the melt produced by the effect of "constitutional liquation". This means the liquation of the matrix due to lowering of the melting point caused by carbon concentration increased by carbon diffusion from graphite grains to the matrix during the process of welding. Hereafter we refer to the section where any ledeburite is found as the "partially-melted zone", and to the section where no ledeburite is found as the "true heat-affected zone".

Figure 8 shows an example of the microstructure of the fractured region of a specimen which was fractured at 405K under the stress of 404.7 MPa and welding heat input of 1.8 kJ/mm. This is a photograph of the fractured part of the backing plate side which was nickel-plated on the face of the fracture, cut longitudinal by an electro-spark machine and ground for microscopic observation. The upper part of the photograph is the composite region side and the lower nickel-plated part is the true heat-affected zone side. Close observation reveals that the fracture occurs at the martensite structure in the true heat-affected zone adjoining the partially-melted zone where nodular graphite grains are surrounded by a ledeburite. Microstructures of the fractured zone show the same pattern regardless of the welding heat input and the specimens with circumferential and spiral notches fracture at the martensite structure, the same as the smoothed specimens do.

Figure 9 shows an example of a SEM image of a fractured section of a smoothed implant specimen fractured at 348K under the conditions of 2.1 kJ/mm of heat input and 278.3 MPa of applied stress. Most

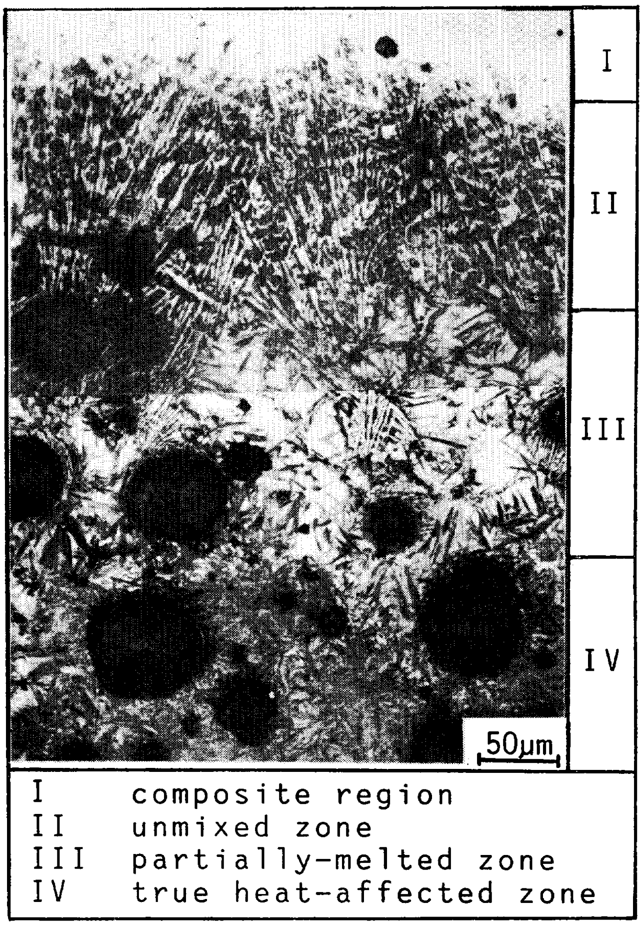

Fig. 7 Microstructure of welds, heat input: 2.1 kJ/mm

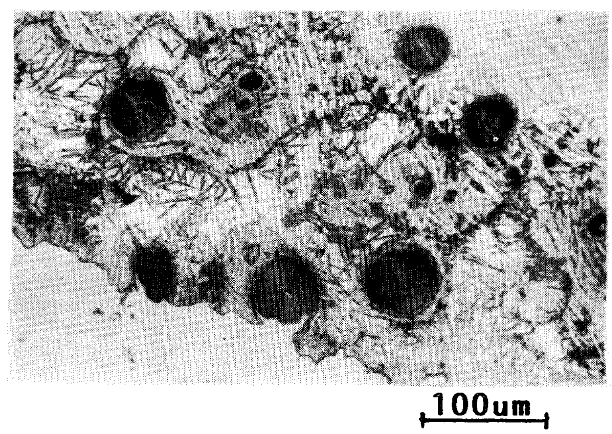

Fig. 8 Microstructure of fractured region

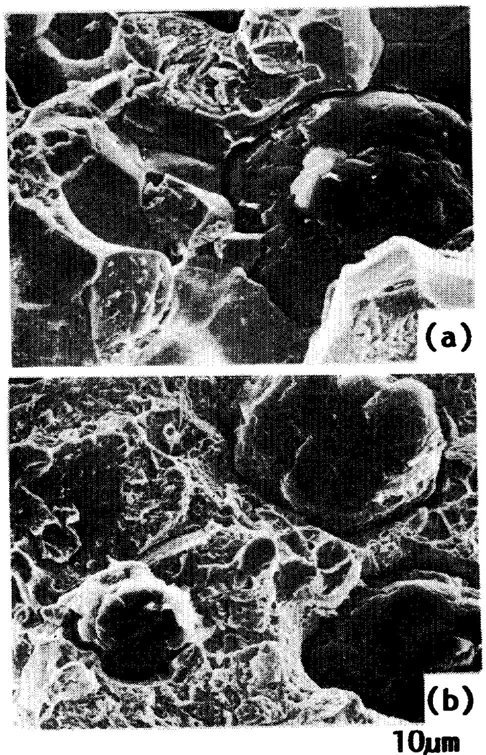

Fig. 9 Fractographs of the specimen fractured at 348K, heat input: 2.1kJ/mm, applied stress: 278 MPa, (a): center, (b): circumference

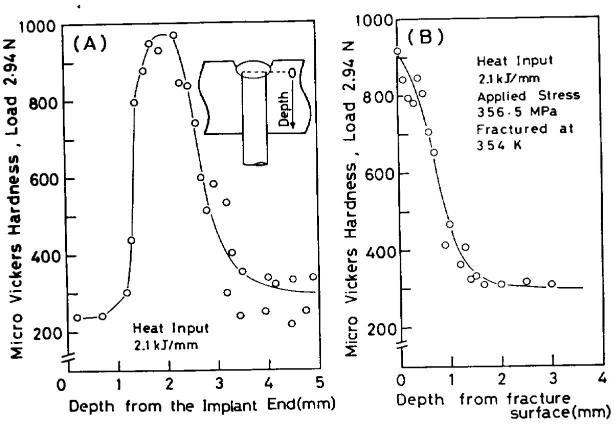

Fig. 10 Hardness distributions of welds (left: A) and fractured specimen (right: B)

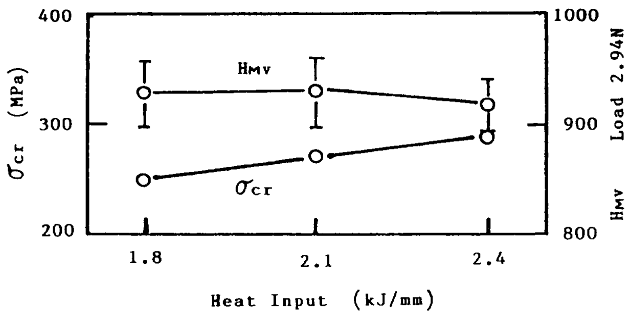

Fig. 11 Effect of heat input on the σ_{cr} and the maximum hardness value of fractured region

of the central area of the fractured part is occupied by intergranular fracture and partly by quasi-cleavage fracture. The circumferential part consists of a wide quasi-cleavage fracture area and a partial intergranular fracture. Black grains in the photograph are nodular graphite and the fractograph shows that almost no plastic deformation is followed by a fracture, which takes place in the martensite structure. This pattern of fracture differs obviously from that of the tension test specimen which contains dimples and river patterns, and it proves itself to be formed by a brittle fracture due to the formation of martensite structure. As the fracture took place instantaneously without preliminary changes, any data that could give information concerning the progression of fracture were not obtained. Even close observation of the fractured section could not detect the starting point of cracking in either the central or circumferential part of the section. Also, the heat-affected zone of the non-fractured specimens was surveyed carefully, but an arrested crack could not be found. These are the problems that remain for future study.

3.3 *Hardness Distribution of the Fractured Region*

Figure 10-(A) and (B) show examples of hardness distribution of the weld zone measured by a micro-Vickers hardness tester, with 2.94 N of testing load. (A) is the diagram for a non-fractured implant specimen, with the origin of the coordinate axes set at the upper end of the specimen. (B) is for a specimen which fractured at 354K under the stress of 356.5 MPa was nickel-plated on the fractured surface. The origin of the coordinate axes is located on the fractured surface in the longitudinal cross section. The diagram (A) shows an abrupt rise in hradness at around 2 mm depth from the implant end. This hard place is located just at the above mentioned weld boundary where the ledeburite solidification and the martensite transformation took place. Good correspondence of the hardness distribution between (A) and (B) diagrams proves that the fracture took place in the structure around the highest hardness zone.

Figure 11 shows the change of critical rupture stress and the hardness at the fractured region according to the change in welding heat input. The hardness of the fractured region has a considerably high value, such as 900 to 950 H_{MV}, with little regard to the change in heat input. As shown in Table 3, the cooling times from 1073K to 773K are 3.9 seconds and 4.9 seconds for the heat input of 1.8kJ/mm and 2.4kJ/mm respectively. The slight difference in cooling time is considered to have no significant influence on hardness, although the critical rupture stress shows a slight increase.

3.4 *Diffusive Hydrogen*

As the implant test of steel is mainly employed in the study of the delayed cracking due to the diffusive hydrogen which tends to accumulate at the stress-concentrated spots, the shape, size and location of notching have been studied and designed such that the fracture takes place at the notch[12]. However it has been reported that the implant test of high carbon steel is not affected much by diffusive hydrogen[13], and another report says that the underwater welding test using nickel core wire electrode accumulates little diffusive hydrogen because the weld metal forms an austenite structure containing much solid solution of hydrogen[14].

To study the effect of diffusive hydrogen on the results of the present work, diffusive hydrogen from the beads of 50 mm length laid with the testing electrode on three pieces of cast iron plate was collected in mercury according to the standard procedure of JIS Z3113. The measurement after 96 hours showed almost no diffusive hydrogen. Based on the result of this test, the authors considered that no hydrogen participated in the cracking of the present study.

3.5 *Estimation of Cracking Susceptibility*

Unlike in the case of steel, the implant test of nodular graphite cast iron proved that the critical rupture stress can be obtained in a specific range of temperatures after the martensite transformation progresses to a certain extent, while a change in the testing load and starting time of the loading has little effect. The fact that the fracture takes place at the high hardness part in the heat-affected zone, and the critical rupture stress rises only slightly as the welding heat input increases, means that the test results have been obtained as an effect of welding.

In the case of steel many reports of weld cracking have been presented, and the implant test has been standardized in WES 1104 as a testing method of cold cracking at the heat-affected zone of steel weld. But in this report no survey is made to find out the correspondence with other weld cracking tests, and no other report of weld cracking test of nodular graphite cast iron to be compared with ours is available at present, so it will raise a problem if we conclude only from the results stated above that the implant test can lead to an estimation of cracking susceptibility of nodular graphite csat iron. Here the authors state only that the critical rupture stress at the heat-affected zone of nodular graphite cast iron can be obtained from the implant test.

4. Conclusions

The following is a summary of the results of an implant test of nodular graphite cast iron of 590 MPa class tensile strength welded with coated arc welding electrode of 55% Ni-Fe base (JIS DFC NiFe) at room temperature.

(1) The implant test can give the critical rupture stress at the heat-affected zone of nodular graphite cast iron.

(2) A fracture of the implant test specimen takes place at about 373K, without regard to the loading start temperature. The temperature at which the fracture takes place shifts slightly to the hotter side as the loading stress increases, but in any case it is lower than the starting temperature of martensite transformation of the specimen, or the fracture takes place after the martensite structure develops to a certain extent. The critical rupture stress increases slightly as the welding heat input shifts from 1.8kJ/mm to 2.4kJ/mm, but in any case it is less than one half of the strength of the base metal.

(3) The fracture takes place at the martensite structure of high hardness in the true heat-affected zone adjoining the partially melted zone. SEM observation of the fractured section reveals that the greater part of the central area of the fractured section consists of intergranular fracture, and most of the circumferential part consists of quasi-cleavage fracture accompanied with no plastic deformation.

(4) As the notch effect of tiny grains of graphite dispersed in the matrix is a dominant factor in cast iron implant testing, no difference between the smoothed specimens and the notched specimens is found, and therefore notching the specimens is not necessary.

Acknowledgments

The authors gratefully acknowledge Dr. Yoneo Kikuta, Professor of Osaka University, for his helpful advices. They also thank Mr. Kohji Miyamoto, a student of the University of the Ryukyus for his cooperative work and thank Welding Research Institute of Osaka University for permitting use of the continuous cooling transformation measuring apparatus. Ductile iron for the study was provided by Okinawa Cast Iron, Inc.

References

1) E.F. Nippes, W.F. Savage and W.A. Owczarski; The Heat-Affected Zone of Arc-Welded Ductile Iron, Welding Journal 39-11 (1969), 465s–472s
2) H. Tamura, N. Kato, S. Yokoi and Y. Ishii; Electroslag Welding of Cast Iron (Report 3), Journal of the Japan Welding Society 43-8 (1974), 794–804 (in Japanese)
3) F. Shibata, S. Ando and N. Fujisaki; Study on the Electron Beam Welding of 50 kgf/mm² Class Nodular Cast Iron, Journal of the Japan Welding Society 51–9 (1982), 748–754 (in Japanese)
4) T. Ohi and M. Fujioka; The Cause of Weld Cracking and Its Prevention during Gas Welding of Cast Iron, Imono (The Journal of the Japan Foundrymen's Society) 51–4 (1979), 206–211 (in Japanese)
5) T. Noguchi; Rupture Strength of Cast Iron Bar with Circumferential Notch, Zairyo (Journal of the Society of Materials Science, Japan) 29–4 (1980), 387–393 (in Japanese)
6) M. Nishida; Stress Concentration, Morikita Pub., (1967), 606
7) H. Granjon; The 'implant' method for studying the weldability of high strength steels, Metal Construction, 1–11 (1969), 505–515
8) F. Matsuda, H. Nakagawa and S. Kato; Study on the Quench Cracking of Weld Heat Affected Zone of High Carbon Steel and Low Alloyed Steel, Preprints of the National Meeting of J.W.S. No. 29 (1981), 266–267 (in Japanese)
9) Y. Toshioka, M. Fukagawa and Y. Saiga; Plasticity of Steels during Martensite Transformation and Quench Cracking in Heat Treatment of Steel, Tetsu-to Hagane (Journal of the Iron and Steel Institute of Japan) 59–2 (1973), 308–312 (in Japanese)
10) F. Matsuda; The Metallurgy of Welding, Nikkan-kohgyo Press, (1972), 196
11) J.J. Pepe and W.F. Savage; Effects of Constitutional

Liquation in 18-Ni Maraging Steel Weldments, Welding Journal 46-9 (1967), 411s–422s

12) Y. Ohkuma; Doctoral thesis, Osaka University, Estimation of Weld Cracking Susceptibility of Steel by Implant Test and Its Application for Selection of Prevention Conditions for Weld Cracking of Heat-Affected Zone on Weld Joint, (1982), 12–28 (in Japanese)

13) F. Matsuda, H. Nakagawa, T. Tsuji and M. Tsukamoto; Effect of Hydrogen Content on Cold Crack Susceptibility of Various Steels with the Implant Test, Transactions of JWRI (Welding Research Institute of Osaka University Japan) 7–2 (1978), 195–201

14) M. Koibuchi and T. Yokota; Underwater Wet Welding with Ni, Fe-Ni and Stainless Steel Electrodes, Journal of the Japan Welding Society, 50–5 (1981), 489–495 (in Japanese)